

## SEDIMENT TRANSPORT INVESTIGATIONS IN A NEW ZEALAND TIDAL INLET

K.P. Black & T.R. Healy  
Department of Earth Sciences  
University of Waikato  
Hamilton, N.Z.

### ABSTRACT

A study of sand and shell movement under the action of tidal flow was initiated in 1980 to ascertain the suitability of Whangarei Harbour at Marsden Point, New Zealand, for a proposed timber port. The aim was to assess the effects such a development may have on the sediment fluxes and the potential shoreline and channel instability that might be induced in the sandy inlet system.

Vertical water velocity profiles were analysed to determine bed friction coefficients which were subsequently broken into two component parts: one due to form drag and the other associated with the skin friction. It was shown that the Vanoni and Hwang (1967) equation for form drag can be extrapolated to include drag under tidal flow over megaripples. The skin friction component was obtained from the speed at 1m above the bed and the  $D_{65}$  grain size, by utilising the Karman-Prandtl equation. This was applied to analysis of bedload trap yields and bedform advance rates over megaripples and good agreement with the Yalin bedload equation for plane beds was obtained.

Suspended sediment transport was found to vary with  $U_1^{7.75}$  and total load rates were in general agreement with the Engelund Hansen equation but deviations occurred due partly to expected form drag components being out of phase with the flow because of bedform hysteresis. Under tidal flow, the velocity at 1m was found to be a better predictor of sediment transport than the shear stress obtained from the velocity profile, thus methods presented in this paper use the 1m speed for determination of total load transport.

### 1. WHANGAREI HARBOUR HYDRAULIC CONDITIONS

Whangarei Harbour (Fig. 1) at high spring tide has a surface area of  $98 \times 10^6 \text{m}^2$  (Millar, 1980) and a tidal prism of  $186 \times 10^6 \text{m}^3$ . At low tide exposed banks cover an area of  $46 \times 10^6 \text{m}^2$ . Currents in the harbour mouth, in depths which exceed 30m attain a maximum vertically-averaged mean speed of approximately  $1.3 \text{ms}^{-1}$  during Spring tides. The channel floors are depleted of sand by these erosive flows and a shell lag lines the bed.

Two flood tidal deltas, Snake and McDonald Banks, possess a high order of stability and the former supports commercial quantities of cockle (*Chione stutchburyi*).

Mair Bank is an ebb tidal delta with several shell beds (Venus and Beazley, 1982) and much of the surficial bank sediment is discarded shell. The bank is protected from ocean wave activity by Busby Head to the east, with generally only E-SE storm waves reaching it with any significant intensity.

Wave activity inside the harbour is mostly locally-generated (fetch  $\sim 5\text{km}$  near the port site) although some ocean swell refracts (Black and Healy, 1981) and diffracts to reach the port vicinity (Fig. 1).

Two continuous-recording tide gauges are located in the harbour; one at Marsden Point near the mouth and the other at Port Whangarei in the upper reaches. Analysis of these records over a seven month period from June to December 1981 revealed that the ebb at the mouth has a shorter average duration of 6 hrs 9 mins compared with the flood average half cycle of 6 hrs 16 mins. Mean tidal range was 1.87m and minimum and maximum ranges were 1.17 and 2.80m respectively.

## 2. COMPLEMENTARY INVESTIGATIONS

General stability of the subtidal deltas and channels was revealed when bathymetric surveys along transects in the lower harbour and across the Mair Bank ebb-tidal delta in 1981 were compared with an R.N.Z.N. survey completed 20 years earlier (1959-61). A complete bathymetric survey by the R.N.Z.N. in late 1981 revealed the same trends. The region of most significant change was on the western end of Mair Bank where sand was accreting. The source for this is most likely to be Bream Bay which has been subject to erosion (Tonkin and Taylor, 1979).

As a first stage in the investigation, some 70 sea floor sites were colour photographed with a still camera (Black et al., 1981) and large areas of shell lag were revealed. Much of the shell was algae-coated signifying bed stability. The photography aided the interpretation and analysis of data collected throughout the study.

A side-scan sonar survey of the inner harbour and Mair Bank region was undertaken in early 1982 (Black and Healy, in preparation, b). The side-scan allowed identification of shell-covered areas and "active" bedload transportation zones which were evident from the megaripples and/or sandwaves on the side-scan traces. Active regions (Fig. 1) flank the main channel where it discharges into Bream Bay. Others occur at Marsden Point and north of Mair Bank; off Pt Sinclair on the south side of the main shipping channel; along the northern side of Snake Bank towards Darch Point then to the west of Reotahi Bay; and finally from the sub-tidal extension south-east of Snake Bank across towards Marsden Point. The last "pathway" runs across the proposed port dredge zone and has been studied in some detail. Other smaller and some less active zones are present. Extensive areas of the harbour bed are covered with shelly lag including a large expanse at the proposed dredge zone. A better understanding of the inter-relationship between these regions is gained in the light of 2-dimensional numerical model results (Black, in preparation).

## 3. MEASURED CURRENT SPEEDS

During a four year period full-tidal cycle velocity measurements were made at 54 sites. These were made at several levels above the sea bed every half hour for a 13 hour period. Sites are shown on Fig. 1 and some were measured twice. This very detailed field program provided an unusually comprehensive specification of the prototype hydraulic conditions.

Using a Braystoke BFM 010 MkII multiparameter meter, the speed, direction, salinity and temperature were recorded at each level. Distance from the sea bed was obtained with a built-in sounder and the meter was winched between levels. At some of the earlier sites, mean velocity was found over a 50s time interval, but to average out the longer period turbulent fluctuations (Dyer 1973; Heathershaw & Simpson 1978) more completely, the recording time was extended to 100 seconds after field tests revealed significant differences (10-20%) in the speeds for two consecutive 50 second intervals.

In obtaining the velocity profile, speeds were measured consecutively, e.g. the speed at an upper level was measured perhaps 15 minutes after the first level. Under normal operation the speeds were measured at each level at half hourly intervals. Parabolæ fitted through three such measurements gave velocity-time curves over a 1 hour period at each level. Instantaneous velocity profiles were determined from these curves.

Without further measurements, turbulent fluctuations with periods of the same order as the measurement time can only be considered as random and as such they cannot be corrected for. Errors introduced by turbulence, which are an integral part of measuring speeds consecutively, must remain in the data. The longer measurement time reduces the scatter considerably.

#### 4. VELOCITY PROFILES

It is well accepted that the Karman Prandtl (K-P) equation describes the velocity profile near the sea bed in the majority of cases for fully rough, turbulent tidal flow. Sternberg (1968) found that a logarithmic profile was evident 62 to 100% of the time over low topography (ripples, gravel and shell). The profile applied in the inner boundary layer, which in fully developed tidal flow is the region from the bed up to about 15-20% of the total water depth. Komar (1976) reported that the outer boundary layer can be described by a velocity defect law (UVDL) of the following form.

$$\frac{U_{\infty} - u}{u_*} = -8.6 \log_{10} \left( \frac{z}{d} \right) \quad \dots (1)$$

$U_{\infty}$  is the free stream speed,  $u$  is the velocity at distance  $z$  above the bed,  $u_*$  is the friction velocity and  $d$  is the boundary layer thickness.

The Karman Prandtl equation can be represented as

$$\frac{u}{u_*} = 5.75 \log_{10} \left( \frac{z}{z_0} \right) \quad \dots (2)$$

where the constant, 5.75, includes the von Karman constant  $\kappa = 0.4$  for conditions of low suspended sediment levels (Soulsby and Oyer 1981) and  $z_0$  is the roughness length. From equations (1) and (2), the friction velocity  $u_*$ , can be found by linear regression. The measured profile gradient on a semi-log plot is  $8.6 u_*$  for the UVDL, and  $5.75 u_*$  for the K-P.

The question arises as to whether the bed shear stress is represented in the body of the flow, under tidal flow conditions. Smith and McLean (1977) state that at great distances from the boundary the velocity field is related "to the overall boundary stress, that is to the boundary stress averaged over a large region of the bed, form drag on the topographic features thus being included". The Whangarei data strongly support this, and values of the drag coefficient are shown to be related to the bed configuration over sand boundaries with megaripples.

Many of the measured vertical profiles spanned the inner and outer boundary layers. It has been shown by Black and Healy (1982b, in prep.) that there is a measurable change in gradient from the inner to the outer boundary layer under tidal flow conditions. At several sites the velocity gradients in the inner layer (taken as 0-20% of the depth) and in the outer layer (taken as 15-100% of the depth) were determined. Although there was considerable scatter for individual profiles, over a tidal cycle the average gradients in the two layers were nearly in the ratio suggested by the UVDL and K-P law of 8.6/5.75. Programming was written to fit the K-P law to the inner layer and the UVDL to the outer layer, then to average the value of the friction velocity obtained from each. This average value was used to calculate the bed shear stress and drag coefficient.

$$\tau_0 = \rho u_*^2 \quad \dots (3) \quad C_1 = \left\{ \frac{u_*}{u_1} \right\}^2 \quad \dots (4)$$

where  $u_1$  is the speed measured at 1m above the bed and  $\rho$  is the water density. Data were not used if fewer than 3 speeds were recorded in either layer.

#### 5. SEDIMENT TRANSPORT EXPERIMENTS

Six full tidal cycle sediment transport experiments were conducted at 3 locations of significance to the harbour sediment circulation (Fig. 1). Measurements were made of water velocities, and both bed and suspended load, while the sea floor was observed on an underwater video camera. A velocity profile (0.5, 1.0,

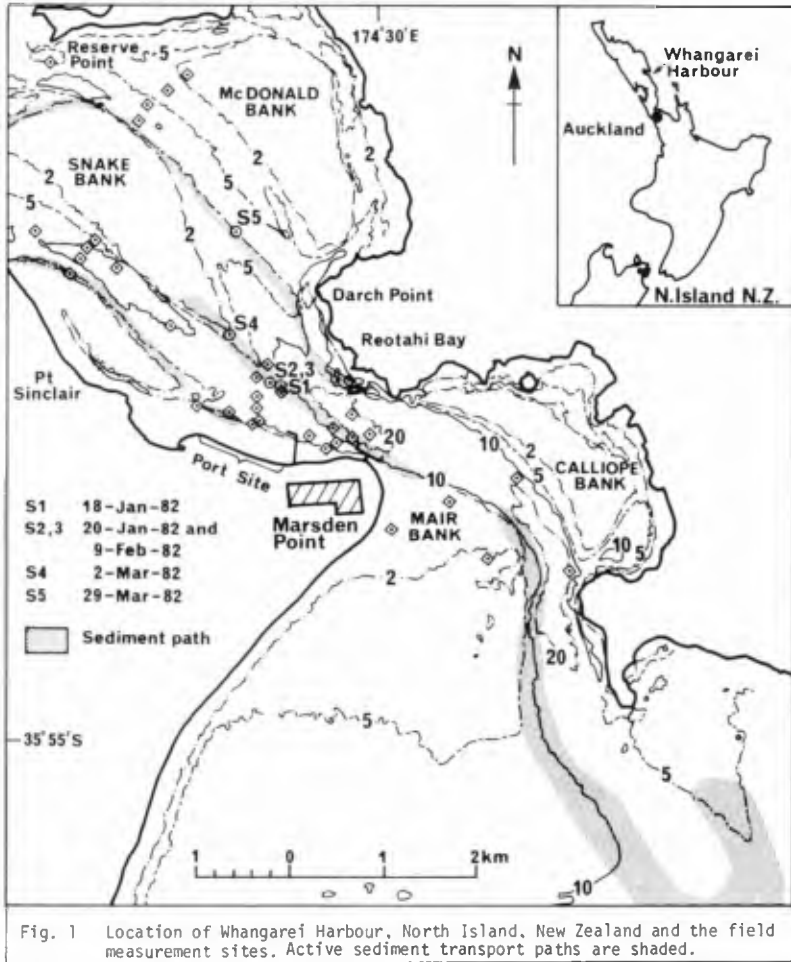


Fig. 1 Location of Whangarei Harbour, North Island, New Zealand and the field measurement sites. Active sediment transport paths are shaded.

2.0, 4.0, 6.0m above the bed) was recorded every half hour (e.g. Fig. 2). Speeds at 1m were measured every 15 minutes or more often on request during periods of interest on the video.

Bedload movement was obtained with two sediment traps of the VUV type (Graf, 1971 p. 363) and emptied every 1-2 hours. The trap is designed to be lowered by rope from the surface but experimentation revealed that a diver was needed to correctly align it on the bed, and to stabilise it in high flow on the way to the surface. Moreover to avoid sand being lost when the trap was raised, a door was fitted to the mouth which could be closed by a diver before retrieval. The traps have a rectangular mouth of size 260mm by 120mm.

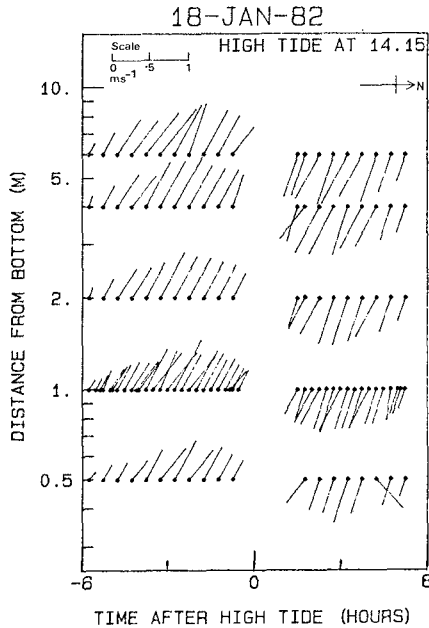


Figure 2: Velocities recorded on 18-Jan-82.  
True North is to the right.

During slack water, stakes were driven into the crests of 6 consecutive megaripples on the bed and crest advance was measured at the next two quiescent periods and during the tide.

Suspended load was sampled regularly at 0.1, 0.3 and 1.0m above the bed by pumping samples to the surface from nozzles mounted on a steel frame.

An underwater video camera mounted on a steel frame on the sea floor, supplied information on the sediment threshold, ripple advance rate and the behaviour of the sediment under tidal flow. Of the 6 experiments the video was used during the first two only.

#### 6. SEDIMENT THRESHOLD

Of fundamental importance to the specification of sediment transport rates are the threshold

conditions which initiate the movement of sediment. Many bedload equations use excess shear stress (Yalin 1963; Sternberg 1972; Bagnold 1963) and small errors brought about by inaccurate threshold conditions are magnified in the transport equations because of a high power dependence. For example, Gadd et al. (1978) modified the Bagnold equation to express the stream power in terms of the velocity at 1m. The bedload was assessed to be proportional to the cube of the difference between the water speed at 1m and the critical velocity.

A major difficulty associated with the determination of threshold in tidal flows is the effect of turbulent fluctuations. Sand moves in gusts, with sweeps and ejections (known as "bursting") occurring intermittently (Heathershaw 1974). When speeds are measured with an instrument such as the Braystoke to produce an average over a period of some 1-2 minutes, these high speed bursts are difficult to incorporate into the concept of a critical velocity. Grass (1970) defined a threshold by considering the overlap of the critical stress distribution associated with the placement of the grain on the bed and with the distribution of bed shear stresses due to fluid flow. Sternberg (1971) defined the threshold as a state of "general sediment movement". In tidal flow even at very low speeds there is still a chance of movement in a burst (Paintal 1971). Dyer (1980) interpreted the threshold as coinciding with the intercept of the regression line of sediment transport against water speed or friction velocity. A statistical approach is adopted in our paper.

#### 6.1 Video Film Over a Sand Bed

The video tapes at Whangarei were analysed in a fashion similar to that undertaken by Dyer (1980). The film was viewed at 5 second intervals and a yes/no decision was made as to whether sandy sediment was moving anywhere in the frame of the camera (approximately a bed area of 12cm x 16cm). From

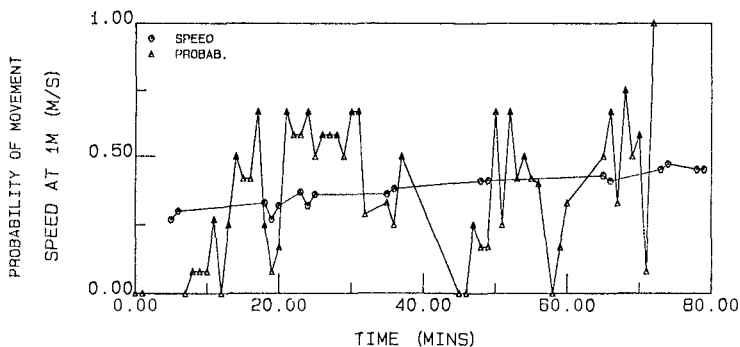


Figure 3: Sandy sediment threshold showing the probability that sand will move in a 1 minute interval with the speed at 1m, for 18-Jan-82 and based on analysis of video tapes.

12 consecutive answers a probability of movement was calculated for the one minute period.

Fig. 3 shows results for one tide during accelerating flood flow plotted with the speeds measured 1m above the bed. Initially below  $0.3 \text{ ms}^{-1}$  no movement was seen. Then firstly, as reported by Dyer (1980), shell fragments move randomly, appearing to "wobble" in the flow. These shell fragments were not considered for Fig. 3, which corresponds with the motion of sand grains only.

Grain size of the sediment viewed was found by sieving samples taken from nearby sediment traps, and off crests and troughs of the megaripples by divers. Median size  $D_{50}$  was coarsest in the troughs ( $0.35\text{mm}$ ); finer in the trap ( $0.32\text{mm}$ ); and finest on the crests ( $0.31\text{mm}$ ). The sand in the trap was felt to best represent the population of sand that was being transported.

Initial motion - such that sand grains were moving more than 50% of the time - occurred when the speed at 1m was between  $0.3$  and  $0.35 \text{ ms}^{-1}$ . This was less than the corresponding threshold for grains over a plane bed (reported in Miller et al. 1977) and calculated to be  $0.45 \text{ ms}^{-1}$ .

The difficulty of assigning a threshold in tidal flow is highlighted by Fig. 3 where, after periods of activity and even with an increase in mean speed, there are still dormant times. Also the probability of movement shows no increase near time = 70 mins compared with time = 25 mins. This suggests that the threshold is increasing with increased flow velocity (Dyer 1980).

## 6.2 Laboratory Flume

In view of the effects on the threshold of the spread of the grain size distribution and the grain shape, experiments were conducted in a rectangular glass walled flume with sand taken from the port site at Marsden Point. The flume was  $0.44\text{m}$  wide and  $12.9\text{m}$  long, and shear stresses were determined by measuring vertical profiles on the centre line  $9\text{m}$  from the top end of the flume with a mini flow meter. The impellor size was  $9\text{mm}$  diameter. Observations of initial motion were made along the centre line and the bed was initially flattened before each run.

Grain size analyses from three sieved samples produced an average mean grain size of  $0.24\text{mm}$ ,  $D_{50}$  of  $0.25\text{mm}$  and standard deviation of  $0.41\phi$ . These statistics were calculated by the moments method from the weight distribution in phi units.

The threshold obtained by curve fitting the vertical velocity measurements to the K-P equation was  $u_* = 0.0148 \text{ ms}^{-1}$  or shear stress  $\tau_o = 0.219 \text{ N.m}^{-2}$ . This is somewhat higher than an expected value of  $u_* = 0.0133 \text{ ms}^{-1}$  (Yalin threshold curve modified by Miller et al. 1977) but is within the range of scatter on Fig. 3 in Miller et al. for quartz density sand of the same mean size, which includes values over the rather wide range of  $0.0125 < u_* < 0.0161 \text{ ms}^{-1}$ .

### 6.3 Shell Bed

A coarse, shelly lag covers large areas of harbour floor and several experiments were conducted on the sea bed watching for the initiation of shell movement.

The difficulty encountered in these observations was due to the wide variety of shape and size of the shells. In summary, the general conclusions were that on a bed of total shell cover even in Spring tides the shells rarely move. Many of the beds have an aged appearance with the shells being covered by algae; a testimony to the stability of the sediment. Shells which were picked up by divers fell quickly to the sea bed and found a stable position with an orientation that depended on the configuration of their immediate neighbours. In contrast, on the sandy harbour floor pelecypod halves prefer to lie convex up but are more stable than surrounding sand.

## 7. ESTUARINE BED FRICTION ENERGY LOSSES

Tidal energy losses over a rough bed are complicated by many factors including flow accelerations and the mutual interaction of the fluid and the bed. Bedforms change with the stage of the tide, and moreover, the time-scale of bed inertia differs from that of the fluid (Allen 1973; Allen and Friend 1976; Nasner 1978). To estimate sediment transport rates under these conditions, the skin friction and form drag energy loss components must be isolated as only the former is effective in transporting sand (Einstein 1950). Whangarei velocity data were fitted by linear regression as described previously to determine the friction velocity (and the associated parameters: bed shear stress, drag coefficient and roughness length) and were then broken into component parts for application to sand transport under oscillatory tidal flow.

### 7.1 Average Bed Resistance

Fig. 4 shows the drag coefficient distribution for all sites (excepting sites discussed individually later) where the speed at 1m from the bed was greater than  $0.3 \text{ ms}^{-1}$ . The minimum speed limit ensures that the flow is fully rough (flow Reynolds Number greater than approximately  $1.5 \times 10^5$  (Sternberg 1968)) and it is a natural cut-off being approximately the entrainment velocity for sandy sediment.

There is scatter of about 5 orders of magnitude in the flood values and 4 for the ebb. This compares with a similar spread found to occur in Chesapeake Bay by Ludwick (1975). Much of this is accounted for by variations in form drag over the wide range of bed types in Whangarei Harbour including sand bedforms, shell, gravel and marine flora.

The distribution peak during the flood lies between  $1.0 \times 10^{-3} < C_1$  (flood)  $< 3.2 \times 10^{-3}$  with the ebb maximum spanning a higher range  $3.2 \times 10^{-3} < C_1$  (ebb)  $< 1 \times 10^{-2}$ . Also the correlation coefficient representing the goodness of fit of the measured profiles to the logarithmic shape was larger during the ebb than the flood (Table 1).

Ludwick (1975) noted a higher drag coefficient on the ebb using the same sort of experimental technique and Knight (1981) found that "in general the flood resistance coefficients were slightly less than the ebb values" in a tidal reach of the Conway estuary. Longitudinal density gradients may be partly responsible for the variations (McDowell and O'Connor, Fig. 1.10 1977).

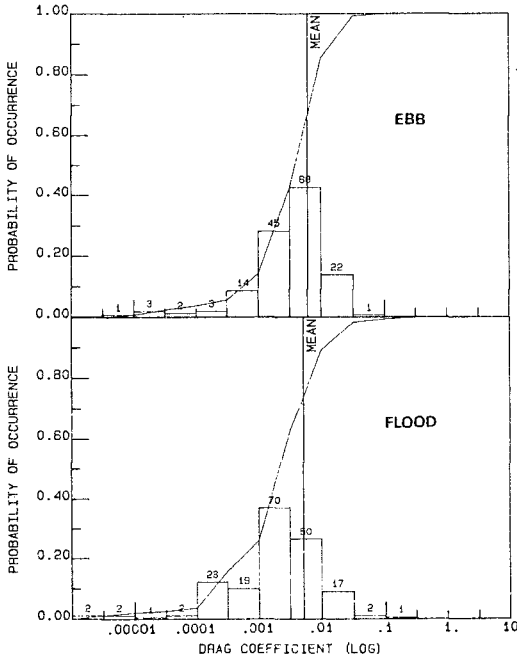


Figure 4: Distributions of ebb (upper) and flood drag coefficients for cases where  $u_1 > 0.3 \text{ m.s.}$  Numbers above bars are the numbers of occurrences in each bin.

The shorter duration of the ebb flow and also the higher water speeds may be an influence.

Table 1 compiles mean statistics for (a) all sites, (b) sites with known shell beds and (c) sites with sand beds for all cases where the velocity at 1m exceeds  $0.30 \text{ ms}^{-1}$ . Mean and median  $C_1$  values are supplied. Arguably, the mean is not the best statistic to describe a distribution which varies over several orders of magnitude. As with grain size analysis, the percentile sizes often represent the distribution and a physical process better than the mean; similarly median  $C_1$  is a more stable statistic which is less affected by a few large  $C_1$  values that may result from experimental error.

Over sand which is presumably bedformed, the increase of friction velocity due to form drag is reflected in a higher  $C_1$  than over the shell sites. Median drag coefficients for cases where  $u_1$  exceeds  $0.3 \text{ ms}^{-1}$  at Whangarei are then  $C_1 = 3.0 \times 10^{-3}$  for all bed types

TABLE 1:

		$\bar{u}_1$ ( $\text{ms}^{-1}$ )	$r_{12}$	$\bar{u}_*$ ( $\text{ms}^{-1}$ )	$\bar{C}_1$ ( $\times 10^3$ )	$\bar{R}$ ( $\times 10^{-6}$ )	Median $C_1$ ( $\times 10^3$ )	$z_o$ $\times 10^2$ (m)
All Sites N = 513	Ebb	0.52	.80	.032	6.0	4.5	3.8	.15
	Flood	0.47	.55	.019	5.1	4.2	2.1	.02
	Both	0.49	.66	.025	5.5	4.3	3.0	.07
Shell Sites N = 132	Ebb	0.52	.73	.026	5.4	4.4	2.7	.05
	Flood	0.46	.31	.012	5.1	3.8	1.8	.01
	Both	0.49	.52	.019	5.2	4.1	2.3	.02
Sand Sites N = 238	Ebb	0.52	.81	.037	6.9	4.7	4.4	.24
	Flood	0.48	.50	.020	6.4	4.3	2.6	.04
	Both	0.50	.65	.028	6.7	4.5	3.5	.12

Mean values of velocity at 1 metre ( $\bar{u}_1$ ), correlation coefficient of the velocities to the logarithmic profile ( $r_{12}$ ), friction velocity ( $\bar{u}_*$ ), drag coefficient  $\bar{C}_1$  and Reynolds Number

$$R = \frac{u_1 z}{\nu}, \nu = \text{kinematic viscosity, } z = 1\text{m.}$$

Median  $C_1$  is listed with the roughness length,  $z_o$ , calculated from the median  $C_1$  using the K-P equation. N is the number of data points averaged.

(c.f.  $3.1 \times 10^{-3}$ , Sternberg 1972);  $C_1 = 2.3 \times 10^{-3}$  for shell bed; and  $C_1 = 3.5 \times 10^{-3}$  for non-cohesive sand bed.

By application of the Student's t test (Freund 1974), for the population correlation coefficient to be significantly different from zero, the sample correlation coefficient must exceed 0.81 for a typical case of 5 velocity measurements in the profile (0.99 for 3 levels) at the 0.05 level of significance. Only 57% of the profiles had  $r_{1,2} > 0.8$  which is poorer correlation than that obtained by Sternberg (1968) and reflects that (i) the outer boundary layer is more subject to inertial variations than the inner layer and (ii) turbulent fluxes cannot be totally accounted for when speeds are measured sequentially.

### 7.2 Friction Losses Over Megaripples

Figs 5 and 6 show velocity at 1m and friction velocity for 5 of the sediment transport sites with megaripple beds. The friction velocity varies over a wider relative range than the speed at 1m. For example the friction velocity on the 9th February 1982 is about 5 times the value on the 20th January 1982. The explanation for this lies with the changing form drag, and sympathetic drag coefficient which is indicative of bed geometry. Dyer (1980) following Lettau (1969) suggests that the areal concentration of features is related to the flow roughness length as,  $z_o = h.s/2S$  where  $h$  is the effective obstacle height,  $s$  is the cross-sectional area seen by the flow per unit horizontal area  $S$ .

For two dimensional megaripples,  $z_o = \Delta^2/2A$ , where  $\Delta$  is the bedform height, and  $A$  is the wavelength.

Insertion of this into the K-P equation produces,

$$C_1 = 1/[5.75 \log_{10} \frac{2A}{\Delta^2}]^2 \quad \dots(5)$$

Average bedform heights and lengths were obtained from measurements at high and low water over 6 consecutive megaripples (Table 3). From this, the expected value of  $C_1$  was calculated with (5) above and the median and mean values from the velocity profiles compared with it (Table 3). The agreement supports the suggestion of Smith and McLean (1977) that the profile reflects the average shear stress over a large region of the bed.

There is an overall correlation of the bedforms measured at slack water to the mean drag coefficient but the friction velocity varies widely throughout the tidal cycle. This compares with similar variations described by Dyer (1970) as "anomalously high and low", and assessed to be associated with the position relative to the megaripple crest at which the profile was measured. For the case at Whangarei where measurements were made largely in the outer boundary layer, the position of the megaripple crest is not as critical and the peak  $u_*$  is possibly related to the time when the megaripples turn around and generally occurs when the 1m speed is  $0.5-0.55 \text{ ms}^{-1}$ .

### 7.3 Form Drag and Skin Friction

In laboratory flumes a logarithmic relationship has been shown to exist which relates the form drag friction factor,  $c''$ , to the geometry of the bed and flow depth (Vanoni and Hwang 1967; Pillai 1979).

The Vanoni and Hwang equation for a 2-dimensional bed can be written as

$$\frac{1}{\sqrt{f''}} = 3.3 \log_{10} \left[ \frac{dA}{\Delta^2} \right] - 2.3 \quad \dots (6)$$

$$\text{and } f'' = \frac{8u_*'^2}{\bar{u}^2} = \frac{8}{c''^2} \quad \text{i.e. } c = \frac{\bar{u}}{u_*'} \quad \dots (7)$$

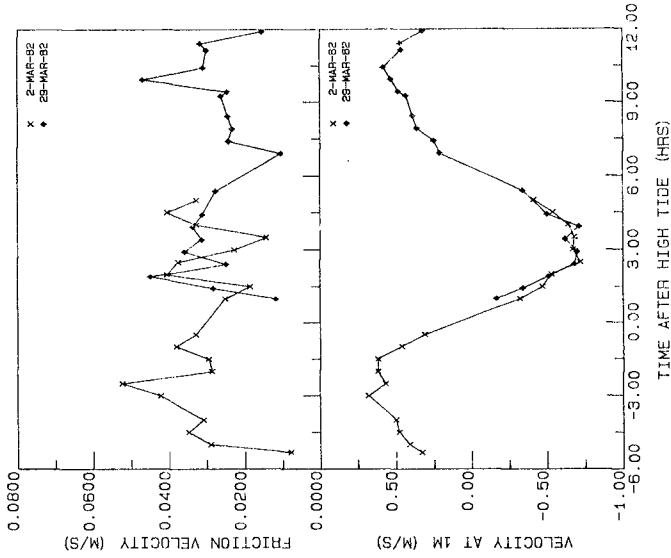


Figure 6: Friction velocity and velocity at 1m above the bed against time after high tide.

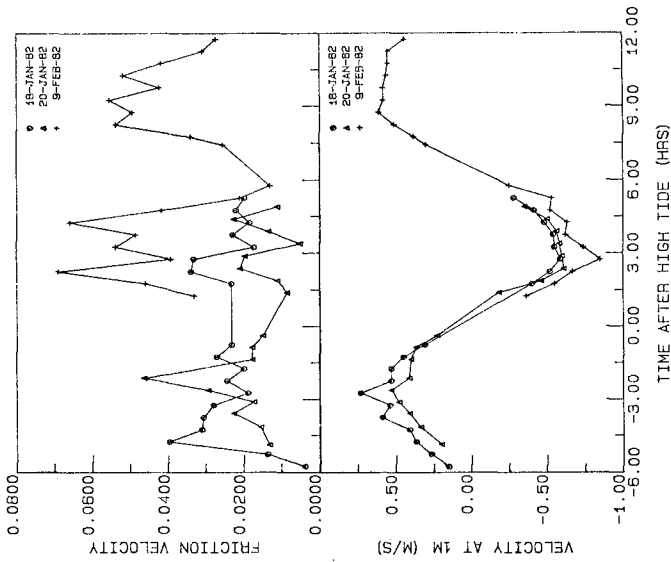


Figure 5: Friction velocity and velocity at 1m above the bed against time after high tide.

$\bar{u}$  is the mean water speed and  $u_*''$  is the friction velocity associated with the form drag, and  $d$  is depth of flow.

As is usual the superscript (") will refer to form drag and the superscript (') will denote association with skin friction. Furthermore, the skin friction factor,  $c'$ , may be derived using the K-P equation as

$$c' = \bar{u}/u_*' = 5.75 \log_{10} \frac{0.38d}{(k_s/730.2)} \quad \dots (8)$$

where mean speed occurs at 38% of the depth,  $d$ , above the bottom and  $k_s$  is the Nikuradse roughness.

Over a moving bed, the roughness can be represented by  $k_s = 2.0 D_{65}$ , where  $D_{65}$  is the grain size for which 65% is finer by weight. This assumes that the K-P equation is valid all the way to the surface, which has been shown to be strictly incorrect but will suffice for the sake of these calculations, (Mehta (1978) suggests that the K-P relationship can be used for determining mean speed in estuaries). If the total bed shear stress is partitioned in a fashion proposed by Einstein and Barbarossa (1952) such that the component due to form drag and that due to skin friction can be summed to give the total shear stress then,

$$u_*^2 = u_*'^2 + u_*''^2 \quad \dots (9)$$

$$1/c^2 = 1/c'^2 + 1/c''^2 \quad \dots (10)$$

$$f = f' + f'' \quad \dots (11)$$

This does not include a third component associated with energy lost by the flow when sediment is suspended (Yalin 1977).

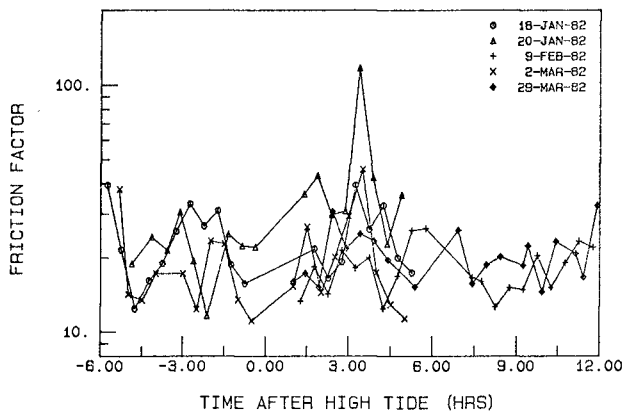


Figure 7: Friction factor ( $\bar{u}/u_*$ ) against time after high tide.

Calculations to determine the combined friction factor from megaripple and grain sizes with eqns (6) and (8) respectively were compiled on Table 4 along with measured values of  $c$  (Fig. 7) found from the mean speed and friction velocity. Table 4 shows that the median measured friction factor is consistently 5-10% greater than the value obtained from the bed parameters. This consistency for average

conditions is very encouraging even though several approximations were made including that (1) the bed geometry measured at slack water is representative of the bed during the tide; (2) a mean water depth taken as the depth at mid-tide is sufficient; (3) the megaripples are 2-dimensional; (4) the  $D_{65}$  grain size represents the bed grain roughness adequately; and (5) the K-P equation can be used to ascertain the skin friction. (Annambhotla et al. (1972) stated that Missouri River data were

TABLE 2:

	Mean depth (m)	D <sub>35</sub> (mm)	D <sub>50</sub> (mm)	D <sub>65</sub> (mm)	D <sub>90</sub> (mm)	T°C	$\theta^1_{Cr}$	$u^*_{*Cr}$	$u''_{*Cr}$	$u^*_{*Cr}$
18-Jan-82	9.0	.28	.30	.32	.39	21	.042	.0140	.0160	.0213
9-Feb-82	8.5	.32	.34	.37	.48	20	.040	.0146	.0213	.0258
2-Mar-82	3.5	.30	.32	.34	.41	20	.041	.0143	.0198	.0244
29-Mar-82	8.5	.20	.24	.27	.44	19	.048	.0133	.0170	.0216

Mean depth, grain sizes, temperature and critical values at threshold of the Shield entrainment function (Yalin curve), skin friction velocity (Yalin curve), form drag friction velocity (Vanoni and Hwang) and the total critical friction velocity.

TABLE 3:

	$\bar{\Delta}$ (m)	$\bar{\lambda}$ (m)	(a)C <sub>1</sub> x 10 <sup>3</sup>	(b) $\bar{C}_1$ x 10 <sup>3</sup>	(c)C <sub>1</sub> x 10 <sup>3</sup>
18-Jan-82	.17	7.5	4.1	3.3	3.4
9-Feb-82	.25	3.7	7.0	6.5	6.3
2-Mar-82	.15	4.6	4.4	4.3	4.4
29-Mar-82	.16	4.2	4.6	4.4	4.1

Mean megaripple height ( $\bar{\Delta}$ ) and wavelength ( $\bar{\lambda}$ ) with (a) predicted drag coefficient (b) measured mean drag coefficient (c) measured median drag coefficient. Data for 18-Jan-82 relies on only one measurement of  $\Delta$  and  $\lambda$ .

TABLE 4:

	C''	C'	C <sub>calc.</sub>	Median C	Deviation
18-Jan-82	25.0	29.9	19.2	21.4	10%
9-Feb-82	18.7	29.4	15.8	17.5	10%
2-Mar-82	20.2	27.4	16.3	17.2	5%
29-Mar-82	23.3	30.2	18.5	19.8	7%

Form drag friction factor C'', skin friction factor C'; total friction factor C<sub>calc.</sub>, calculated from C'' and C'; measured median friction factor; and percentage deviations between calculated and measured C.

TABLE 5:

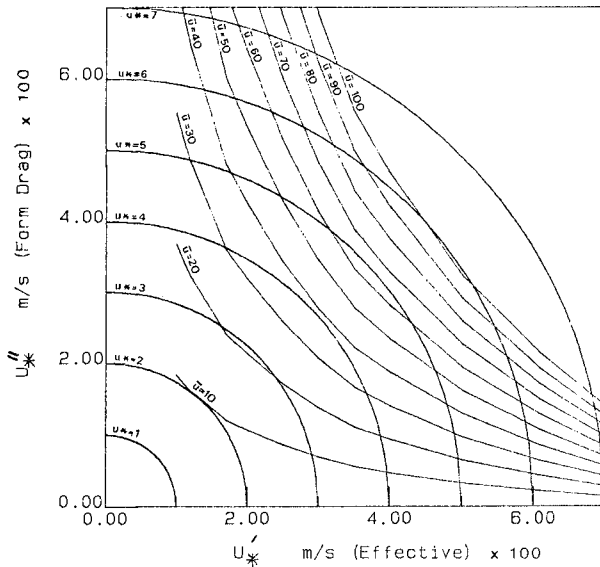
Date	Time	Z	Z <sub>m</sub>	$\alpha$	$u_*$	C <sub>1,0m</sub>	u <sub>1</sub>	$\bar{u}$
9-Feb-82	10.35	1.38	.70	1.20	.0610	8.52	.77	.94
	12.06	1.53	.33	1.46	.0554	17.51	.68	.94
	17.20	1.52	.60	1.28	.0557	.91	.57	.80
2-Mar-82	18.37	1.71	-.08	-	.0497	2.52	.61	.79
	9.19	2.00	.94	1.21	.0394	2.63	.65	.73
	11.12	2.28	.68	1.35	.0346	4.62	.60	.61
29-Mar-82	15.09	2.42	.84	1.31	.0326	13.81	.78	.72
	13.20	1.47	.66	1.20	.0348	6.95	.71	.78
	15.11	1.65	.24	1.50	.0309	3.60	.62	.56
	21.31	1.73	.65	1.25	.0295	4.64	.47	.66

Suspended sediment statistics: defined as z, calculated Rouse number (eqn 16); Z<sub>m</sub>, regressed Rouse number;  $\alpha$ , fall velocity power;  $u_*$  (ms<sup>-1</sup>) friction velocity; C<sub>1,0m</sub>, (kg.m<sup>-3</sup> x 10<sup>3</sup>) concentration of sediment as mass per unit volume at 1m; u<sub>1</sub>, (ms<sup>-1</sup>) speed at 1m;  $\bar{u}$ , (ms<sup>-1</sup>) mean speed.

"reasonably consistent" with the Vanoni and Hwang equation for a similar range of the function  $\Delta^2/(Ad)$ .

It appears that the form drag losses can be estimated adequately with the Vanoni and Hwang equation under tidal flow. Similar calculations made with the Engelund and Hansen (1967) development, which employs Carnot's equation for sudden flow expansions, produced unrealistically high values of the form drag friction factor in depths of 8-10m.

Furthermore, the Einstein-Barbarossa (1952) division of form drag and skin friction (Fig. 6.13, Raudkivi 1976), which relies on an implicit assumption that the mean flow and the bedforms are in equilibrium, was found to be unworkable for tidal flow where the bed hysteresis introduced a complicating factor, such that the bed geometry depends on the history of the bed as much as on the present conditions. Fig. 8 presents the Einstein-Barbarossa method in a site specific format. By entering this figure with the mean speed and friction velocity, the intersection of the two curves should supply the magnitudes of  $u_*'$  and  $u_*''$ . In many cases with Whangarei data, it was found that the  $u_*'$  and  $u_*''$  curves did not intersect and no solution was possible especially near the beginning or end of the tide.



8. BEDLOAD TRANSPORT OVER MEGARIPPLES

The bedload transport rates indicated by trap yields were compared with empirical equations derived from unidirectional flow data, to ascertain their applicability to the tidal environment in a megarippled region.

Of the six sediment transport experiments, three days were rejected (a) for wave interference or (b) because only one bedload trap was serviced. On the remaining three days, two traps were deployed simultane-

Figure 8: Einstein-Barbarossa division of form drag and skin friction for  $D_{35} = 0.0002m$ ,  $\rho_s = 2650 \text{ kg.m}^{-3}$ ,  $\rho = 1025 \text{ kg.m}^{-3}$ .

ously and the weights caught were averaged. This accounts in part for variations of transport rate with position on the bedform. Accepting Graf's (1970) assessment of work by Novak that VUV traps are about 70% efficient the trapped weights were scaled accordingly to compensate for systematic deficiencies.

In all cases, the bedload traps were placed for 1-2 hours and during this time both the friction velocity and  $lm$  speed varied so that an "average" value had to be found. To do this, the area under the curves of velocity versus time was ascertained numerically by finding the area under continuously updated parabolae fitted to three values of velocity; the one nearest the time of interest

and the one before and after. Because bedload equations are non-linear in  $u_*$ , and vary as  $u_*^3$  according to the Yalin equation, when a representative friction velocity was required, the interpolated values were cubed to ascertain the area under the cube of the function between the times that the traps were submerged. The resulting friction velocity was the cube root of the area divided by the elapsed time. With the cubed refinement, an improved correlation to the Yalin equation was obtained (Black, in preparation). By a similar method the Engelund Hansen predicted transport rate, was found from the area under the function  $u_*^2 \cdot u_*^3$ .

It was necessary to introduce a critical friction velocity because often the traps were placed just after slack water in readiness for the next tide, and the total time that the trap was submerged included periods when the bed was dormant. The transport rates and mean friction velocities are more correctly estimated from the time that the bed was in motion. Critical skin friction velocity was found from the Yalin threshold curve (Miller et al. 1977). For cases dealing with total friction velocity, the threshold was the summation according to eqn (9) of the skin friction component from the Yalin curve and the form drag component, which in the light of the analysis in this paper, was calculated from the bedform geometry measured at slack water with the Vanoni and Hwang equation (6). The results of these calculations are compiled on Table 2. In all cases the  $D_{50}$  grain size was assumed to represent the bed sediment.

The data were compared with the Engelund Hansen total load equation for "duned" beds (Engelund and Hansen 1967). In mass per unit width of bed per unit time,  $q_m$ , this is

$$q_m = \frac{0.05 \rho_s}{\left[ g \left( \frac{\rho_s}{\rho} - 1 \right) \right]^2} \cdot \frac{u_*^2 \cdot u_*^3}{D_{50} f} \quad \dots(12)$$

where  $\rho_s$  is sediment density, and  $g$  is the gravitational acceleration. After sieving sediment samples taken from the bedload traps (Table 2) the  $D_{50}$  fall velocity was obtained from the median diameter (Engelund and Hansen 1967, Table 2.2.1).

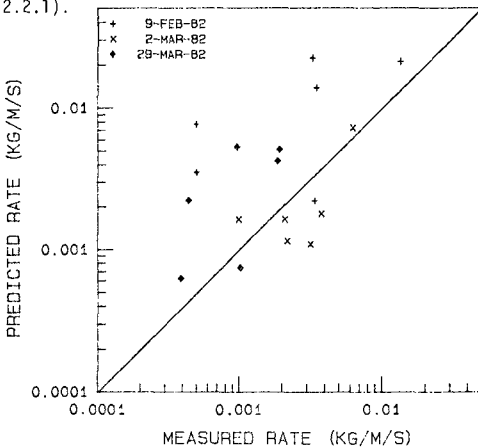
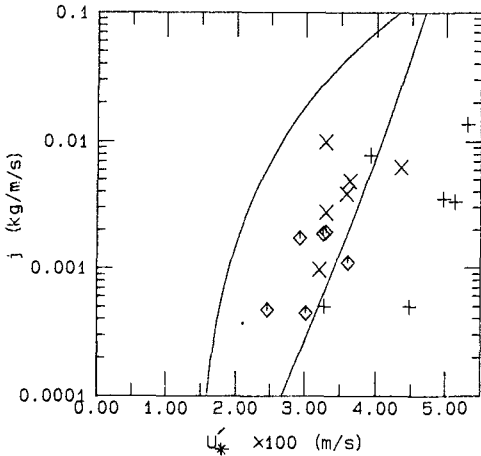


Figure 9: Transport rate according to the Engelund Hansen (1967) total load equation against the bedload trap measured rate.

Fig. 9 shows the predicted rate against the rate determined from the bedload catches. In general, the Engelund Hansen equation overestimates the bedload rate. This would be expected for a total load equation especially at the fastest site on 9th February 1982 where suspended loads which have not been included are likely to be significant. For some cases though (2nd March 1982 especially) there were greater catches in the bedload traps alone than predicted by the total load equation. This deviation is apparently systematic.



On Fig. 10, the transport rates plotted against  $u_{*c}$  were compared with both the Yalin (1963) equation and the Sternberg (1972) modified Bagnold equation. The Yalin equation is for a plane bed and as the friction velocity includes the form drag, which does no effective work on the sediment, the equation overestimates the transport rate in all cases. The Sternberg formula which was partly derived from field data over ripples, approximates the Whangarei data better, but there is still a considerable scatter especially for the cases of high drag coefficient on 9th February 1982.

Figure 10: Measured bedload transport rate against the friction velocity, plotted with the Yalin and Sternberg bedload equations for  $D=0.0003m$  and  $u_{*c}'=0.014 m.s^{-1}$ .

Because of bedform hysteresis and site dependent form drag components, bedload equations which use total bed shear stress are susceptible to inaccuracies in tidal flow because there can be no way of guaranteeing that the effective shear will be represented in the total friction velocity which often has an over-riding form drag component. For this reason, it is felt that a better approach is to attempt to isolate the skin friction (Vittal et al. 1973) and revert to a bedload equation such as the Yalin curve.

Nasner (1978) states that "for water depth of approximately 10m ... the dune height is governed by the ... velocity over the dune crest". The sediment transport rate is similarly motivated, and further analysis revealed that the speed at 1m showed the best correlation with the bedload catches. Returning to the K-P equation, the skin friction was calculated as

$$u_*' = u_1/5.75 \log_{10} \left( \frac{30.2}{k_s} \right) \quad \dots(13)$$

with the roughness selected to be  $k_s = 2.0 D_{65}$ . On Fig. 11 the bedload transport rate is plotted against the derived skin friction. The result is good correlation to the Yalin bedload equation with no apparent systematic deviations related to ebb or flood, or accelerating or decelerating flow (Gordon 1975). The remaining scatter in the data could be due to:

- (i) Bedload trap deficiencies and too few sampling locations on the megaripples.
- (ii) Turbulence at near bed levels which varies with megaripple geometry and is not accounted for by the analysis method. Turbulence over bedforms can affect transport levels especially at the point of flow reattachment (Raudkivi 1976). Turbulence can also reduce the critical friction velocity.
- (iii) Experimental errors related to long term turbulence and the position of the current meter relative to the bedform crest when speeds were measured.

The Yalin bedload equation is:

$$q_m = 0.635\rho_s Du_*^3 [\tau_* - \frac{1}{a} \ln(1 + \tau_* a)] \dots (14)$$

$$\tau_* = \frac{u_*'^2}{u_{*cr}'^2} - 1, \quad a = \frac{2.45\sqrt{6} \tau_{*cr}}{(\rho_s/\rho) D^{1/4}}, \quad \theta_{*cr}' = \frac{\rho u_{*cr}'^2}{(\rho_s - \rho) g D}$$

$\tau_*$  is the dimensionless excess shear stress;  $u_{*cr}'$  is the threshold friction velocity to be ascertained from the Yalin threshold curve, and  $\theta_{*cr}'$  is the threshold Shields entrainment function, and  $D$  is grain size. The application of this equation has advantages in that the rate of transport depends on easily measured quantities, reducing fundamentally to a determination of the speed at  $1m$  and the  $D_{50}$  and  $D_{65}$  grain sizes to specify the bedload rate. This compares with the modification of the Bagnold equation by Sternberg (1972) and by Gadd et al. (1977), for similar reasons. The correlation to the Yalin equation suggests that in oscillatory tidal flow over the short term (1-2 hours), the bedload transport rates approximate their counterparts under unidirectional currents.

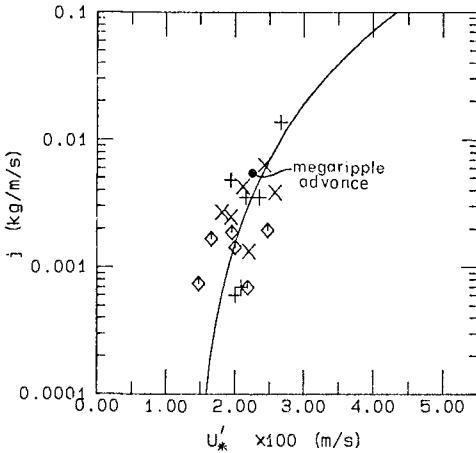


Figure 11: Measured bedload transport rate against the skin friction, plotted with the Yalin bedload equation for  $D=0.0003m$  and  $u_{*c}'=0.014 m.s$

8.1 Megaripple Advance Rates

The experiments with staked megaripple crests were designed to measure nett bedload movement over a tidal cycle. For this reason, the crests were staked and generally measurements were taken at slack water only. It is evident that in reversing flow, it is difficult to estimate the bedload transport rate over a half cycle because when the megaripples turn around, the crest movement is often far in excess of the movement of the centre of mass of the feature, and the latter is required to specify the transport rate. A complete set of measurements over 6 megaripples were taken during the tide (i.e. after the crests

had turned around) and then again at slack water when the features still faced the same way. Only this data is discussed here.

The bedload transport rate was found by application of the method with constants proposed by Engel and Lau (1981), which allows for reverse transport rates in the lee of the bedform crest, and under the assumption that the megaripples were triangular in form. The 6 megaripples (Table 2) moved an average of  $0.3m$  in  $1\frac{1}{2}$  hours when the speed at  $1m$  averaged  $0.53 ms^{-1}$ . When plotted on Fig. 11 the megaripple advance rate compares favourably with both the Yalin bedload equation and the bedload trapping results. Skin friction was assessed with the K-P equation as described for the bedload traps.

9. SUSPENDED SEDIMENT LOAD

Suspended load concentrations have often been described by the Rouse (1937) formula

$$\frac{C}{C_a} = \left[ \frac{d-y}{y} \cdot \frac{a}{d-a} \right]^z \dots (15)$$

where  $C$  is the concentration ( $\text{kg.m}^{-3}$ ) at  $y$  metres above the sea bed;  $C_r$  is the reference concentration at  $a$  metres; and  $d$  is the total water depth. The Rouse number  $z$ , is defined as

$$z = \frac{w}{\kappa u_*} \quad \dots(16)$$

where  $w$  is the fall velocity. Raudkivi (1976) suggests that for small values of  $z$  the formula gives "surprisingly" good results but for larger Rouse numbers there are deviations. Measured Rouse numbers are mostly less than the value calculated by eqn (16) (Fukuoka, Fig. 9.1 1978), signifying a more uniform sediment distribution than predicted by the Rouse formula. The formula could not be applied at Whangarei without modification to  $z$ .

Suspended sediment load was sampled at 0.1m, 0.3m, and 1.0m above the bed from three nozzles mounted on a steel frame. In megarippled regions, the definition of the zero bed level becomes important when sampling heights are comparable to the megaripple height. Also at low levels, the suspended load varies more markedly with distance from the crest. Practical difficulties prevented samples being taken along the length of the bedforms. The stand remained in place for the tidal cycle except to be turned around just after slack water to face into the next tide. For these reasons, the concentration at the highest level i.e. at 1m above the bed, was chosen as a reference.

Samples of approximately 2 litres were passed through a 70 micron filter. Material was washed to remove all fine suspended matter which was not of interest to this study. As no grain size analyses were performed,  $D_{35}$  from the samples out of the bedload traps was selected to represent the material in suspension.

With data from the three levels, the measured Rouse number,  $z_m$ , was found by linear regression, and in all cases (Table 5) it was less than the value from eqn (16), but was generally within the range of scatter in Fukuoka (1978). It was found that the observed concentrations could be predicted with the Rouse formula, when the Rouse number was redefined as,

$$z = \frac{w^x}{\kappa u_*} \quad \dots(17)$$

where  $x$  (Table 5) is any power. Average values of  $x$  were found to be

$$\begin{aligned} \bar{x} &= 1.31 \quad 9\text{-Feb-82} \quad N = 3 \\ \bar{x} &= 1.29 \quad 2\text{-Mar-82} \quad N = 3 \\ \bar{x} &= 1.32 \quad 29\text{-Mar-82} \quad N = 3 \end{aligned}$$

with overall mean of  $\bar{x} = 1.31$ .

The suspended transport rate as mass per unit width of bed per unit time is equal to the integral over the depth of the concentration multiplied by the water speed. To evaluate this, the speeds at 0.1 and 0.3m were found from the gradient of the velocity profile and actual concentrations were used. In the upper levels where speeds had been measured, concentrations were derived from the Rouse formula with Rouse number defined by eqn (17) and  $x = 1.31$  in all cases. The integral was evaluated from 0.12m above the bed (the height of the sediment trap mouth) up to the surface by numerical integration, assuming linear changes between measured levels.

Whereas suspended load showed scatter against  $u_*$  and  $\bar{u}$ , the calculated transport rate when plotted against the speed at 1m (Fig. 12) exhibited good correlation. The best fit equation was

$$q_{SS} = (2.03u_1)^{7.75} \times 10^{-3} \quad \dots(18)$$

where  $q_{SS}$  has units  $\text{kg.m}^{-1}.\text{s}^{-1}$  and  $u_1$  has units  $\text{ms}^{-1}$ .

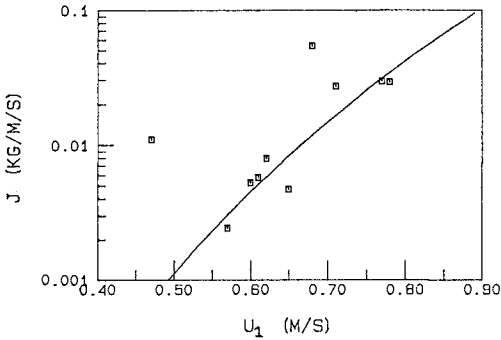


Figure 12: Suspended sediment mass transport rate against the speed at 1m with best fit curve.

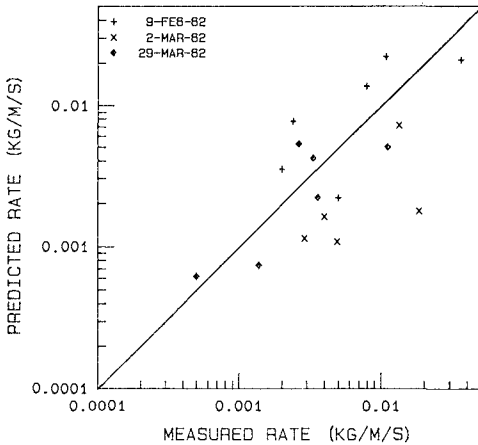


Figure 13: Predicted total load transport rate according to the Engelund Hansen equation against the measured total load transport rate.

The correlation coefficient was 0.94. This equation was obtained with 8 data points and did not include the two points furthest from the curve on Fig. 12. The high power dependence compares with a suspended transport rate proportional to the friction velocity raised to the seventh power found by Dyer (1980).

Applying error bars to the sample correlation of 0.94, with the Fisher Z transformation (Freund 1974, p. 428), the population correlation coefficient lies in the range  $0.70 < R < 0.99$ , at the  $\alpha = 0.05$  level of significance. On the strength of this correlation, which includes data from three sites with different grain sizes, the suspended loads for the periods when the traps were on the bed were found: (1) from each measured velocity at 1m, the suspended sediment transport rate was determined with eqn (18), (2) the mean rates during the bed-load trapping periods were found numerically, (3) these were added to the bedload trap rates and the total load was compared with the prediction of the Engelund Hansen equation on Fig. 13. The comparison is now adequate with data for 9-Feb-82 and 29-Mar-82 showing good correlation.

For the shallow site (2-Mar-82), there is a consistent trend for the measured rate to exceed the prediction by a factor of about 3. Raju et al. (1981) found that the Engelund Hansen equation underestimated the total load by an average factor of about 2 in unidirectional flow. At Whangarei, the deviation is associated with wide variations of friction velocity during the tidal cycle. The plotted point which deviates the most corresponds with an anomalously low friction velocity at about 3 hrs after high tide (Fig. 6). The form of Fig. 6 shows a strong resemblance to flood case (a) of Fig. 6 in Dyer (1970), which is typified by a steep peak ( $u_* > 0.06 \text{ ms}^{-1}$ ) then a sudden drop to an extremely low value of less than  $0.02 \text{ ms}^{-1}$ . Irrespective of whether these variations result from position relative to the megaripple crest or are associated with megaripple reversal, they make it more difficult to determine sediment transport with the bed shear stress obtained from the profile curvature. The

correlation of the  $1m$  speed to the transport rates is pleasing because the former is an easier parameter to determine than either the bed shear stress or the mean velocity.

In summary, with the speed at  $1m$  the suspended load was found from eqn (18), and the bedload with the Yalin equation (14) and skin friction from the K-P relationship (13) with  $k_s = 2.0 D_{65}$ . The variation in grain size for the three sites discussed was  $0.24 < D_{50} < 0.34$  with quartz density of  $2650 \text{ kg.m}^{-3}$ .

#### 10. CONCLUSIONS

(1) Although the drag coefficient varies over several orders of magnitude, it centres on a peak between 0.001 and 0.01 with median value of 0.003 (c.f. 0.0031, Sternberg, 1972).

(2) In tidal estuaries, the form drag over megaripples can be described by the Vanoni and Hwang (1967) equation, and the skin friction by application of the K-P equation with the  $1m$  speed, and the  $D_{65}$  grain size.

(3) As a result of the conclusions in (2), the bedload transport rate was estimated from the effective drag as represented by the skin friction. Bedload trap catches and megaripple advance showed good agreement with the Yalin (1963) bedload equation, which suggests a convenient way to ascertain the bedload transport rate in reversing flow.

(4) Suspended sediment transport rate varied with the 7-8th power of the speed at  $1m$  (correlation of 0.94).

(5) The Engelund and Hansen total load equation adequately described the sediment transport over megaripples at two deeper locations but showed a systematic deviation at a shallower site. This is most likely due to megaripple hysteresis and difficulties associated with determination of effective bed shear stress from the friction velocity in tidal flow. The  $1m$  speed showed better correlation with the transport rates. Use of the  $1m$  speed overcomes the problems inherent in the estimation of  $\tau_0$  from the velocity profile.

#### 11. ACKNOWLEDGEMENTS

This research was undertaken on behalf of the Northland Harbour Board and their considerable assistance and logistic support is gratefully acknowledged. We are also indebted to the R.N.Z.N. for their assistance with the underwater video recording, photography and side scan sonar survey. Dr Alex Sutherland, Civil Engineering, University of Canterbury, kindly read a draft and provided helpful criticisms. A special thanks to our typist for handling a difficult manuscript.

#### 12. REFERENCES

- Allen, J.R.L. (1973): Phase differences between bed configuration and flow in natural environments and their geological relevance. Sedimentology, 20: 323-329.
- Allen, J.R.L. and Friend, P.F. (1976): Relaxation time of dunes in decelerating aqueous flows. Jnl. Geol. Soc. Lond., 132: 17-26.
- Annambhotla, V.S.S., Sayre, W.W. and Livesey, R.H. (1972): Statistical properties of Missouri River bedforms. Proc. A.S.C.E., 98 (MW4): 489-510.
- Bagnold, R.A. (1963): Mechanics of marine sedimentation. In: M.N. Hill (Ed). The Sea, 3. Wiley-Interscience, New York. pp. 507-582.
- Black, K.P. (in prep.): Ph.O. Thesis, University of Waikato.

- Black, K.P. and Healy, T.R. (1981): Computer programs for wave analysis; wind wave generation; wave refraction diagrams; and fast Fourier analysis. Occasional Rept. No. 6, Dept. of Earth Sciences, University of Waikato. 76pp.
- Black, K., Healy, T., Venus, G., Stoakes, J. and Hunter, M. (1981): Marsden Point Forestry Port Investigation, Sea Floor Photographic Survey. Northland Harbour Board. 149pp.
- Black, K.P. and Healy, T.R. (in prep., a): Side-scan sonar survey of the entrance to Whangarei Harbour. Marsden Point Forestry Port Investigation.
- Black, K.P. and Healy, T.R. (in prep., b): On the choice of a boundary layer velocity profile for estuaries.
- Dyer, K.R. (1970): Current velocity profiles in a tidal channel. Geophys. Jnl. Royal Astro. Soc., 22: 153-161.
- Dyer, K.R. (1973): Estuaries : a physical introduction. John Wiley & Sons. 140pp.
- Dyer, K.R. (1980): Velocity profiles over a rippled bed and the threshold of the movement of sand. Est. Coast. Mar. Sci., 10: 181-199.
- Einstein, H.A. (1950): The bedload function for sediment transportation in open channel flows. Tech. Bull. No. 1026, U.S. Dept. Agriculture.
- Einstein, H.A. and Barbarossa, N.L. (1952): River channel roughness. Trans. A.S.C.E., 77: 1121-1146.
- Engel, P. and Lau, Y.L. (1981): Bedload discharge coefficient. Proc. A.S.C.E., 107 (HY11): 1445-1454.
- Engelund, F. and Hansen, E. (1967): A monograph on sediment transport in alluvial streams. Technisk Vorlag, Copenhagen. pp. 62.
- Freund, J.E. (1974): Modern elementary statistics. (4th edn). Prentice/Hall. 532pp.
- Fukuoka, S. (1978): Interaction between turbulent fluid and suspended sediments. Chapter 9 in H.W. Shen and H. Kikkawa (Eds): Application of stochastic processes in sediment transport. Water Resources Publications, Colorado, U.S.A..
- Gadd, P.E., Lavelle, J.W. and Swift, D.J.P. (1978): Estimates of sand transport on the New York shelf using near-bottom current-meter observations. Jnl. Sed. Pet., 48: 239-252.
- Gordon, C.M. (1975): Sediment entrainment and suspension in a turbulent tidal flow. Mar. Geol., 18: M57-M64.
- Graf, W.H. (1971): Hydraulics of sediment transport. McGraw-Hill, 513pp.
- Grass, A.J. (1970): The initial instability of fine sand. Proc. A.S.C.E., 96 (HY2): 619-631.
- Heathershaw, A.D. (1974): "Bursting" phenomena in the sea. Nature, 248: 394-395.
- Heathershaw, A.D. and Simpson, J.H. (1978): The sampling variability of the Reynolds stress and its relation to boundary shear stress and drag coefficient measurements. Est. Coast. Mar. Sci., 6: 263-274.

- Knight, D.W. (1981): Some field measurements concerned with the behaviour of resistance coefficients in a tidal channel. Est. Coast. & Shelf Sci., 12: 303-322.
- Komar, P.D. (1976): Boundary layer flow under steady unidirectional currents. Chapter 7 in: D.N. Stanley and D.J.P. Swift (Eds): Marine sediment transport and environmental management. John Wiley. 602pp.
- Lettau, H. (1969): Note on aerodynamic roughness - parameter estimation on the basis of roughness-element description. J. App. Met. 8: 828-832.
- Ludwick, J.C. (1975): Variations in the boundary drag coefficient in the tidal entrance to Chesapeake Bay, Virginia. Mar. Geol., 19: 19-28.
- McDowell, D.M. and O'Connor, B.A. (1977): Hydraulic behaviour of estuaries. Macmillan. 292pp.
- Mehta, A.J. (1978): Flow dynamics and nearshore transport. Chapter 3 in P. Bruun: Stability of tidal inlets, Elsevier, pp. 83-203.
- Millar, A.S. (1980): Hydrology and surficial sediments of Whangarei Harbour. M.Sc. Thesis, Univ. of Waikato, 212pp.
- Miller, M.C., McCave, I.N. and Komar, P.D. (1977): Threshold of sediment motion under unidirectional currents. Sedimentology, 24: 507-527.
- Nasner, H. (1978): Time-lag of dunes for unsteady flow conditions. Proc. 16th Conf. on Coastal Engineering, pp. 1801-1817.
- Paintal, A.S. (1971): A stochastic model for bed load transport. Jnl. Hydraulic Research, 9: 527-553.
- Pillai, C.R.S. (1979): Effective depth in channels having bed undulations. Proc. A.S.C.E., 105 (HY1): 67-81.
- Raju, K.G.R., Garde, R.J. and Bhardwaj, R.C. (1981): Total load transport in alluvial channels. Proc. A.S.C.E., 107 (HY2): 179-191.
- Raudkivi, A.J. (1976): Loose boundary hydraulics (2nd edn). Pergamon. 397pp.
- Rouse, H. (1937): Modern conception of the mechanics of turbulence. Trans. A.S.C.E., 102: 463-505.
- Smith, J.D. and McLean, S.R. (1977): Spatially averaged flow over a wavy surface. Jnl. Geophysical Res., 82: 1735-1746.
- Soulsby, R.L. and Dyer, K.R. (1981): The form of near-bed velocity profile in a tidally accelerating flow. Jnl. Geophysical Res., 86: 8067-8074.
- Sternberg, R.W. (1968): Friction factors in tidal channels with differing bed roughness. Mar. Geol., 6: 243-260.
- Sternberg, R.W. (1971): Measurements of incipient motion of sediment particles in the marine environment. Mar. Geol., 10: 113-119.
- Sternberg, R.W. (1972): Predicting initial motion and bedload transport of sediment particles in the shallow marine environment. In D.J.P. Swift, D.B. Duane and O.H. Pilkey (Eds): Shelf Sediment Transport. Dowden, Hutchinson and Ross, pp. 61-82.

- Tonkin & Taylor Ltd, Consulting Engineers (1979): New Zealand Electricity Report on Foreshore Erosion Marsden Power Stations, Bream Bay, March 1979.
- Vanoni, V.A. and Hwang, L.S. (1967): Relation between bed forms and friction in streams. Proc. A.S.C.E., 93 (HY3): 121-144.
- Venus, G. and Beazley, M. (1982): The influence of shells on the stability on the north side of Mair Bank. Northland Harbour Board Rept., 41pp.
- Vittal, N., Ranga Raju, K.G. and Garde, R.J. (1973): Sediment transport relations using concepts of effective shear stress. International symposium on river mechanics, Int. Assoc. Hydraulic Research, 1: 489-499.
- Yalin, M.S. (1963): An expression for bedload transportation. Proc. A.S.C.E., 89 (HY3): 221-250.
- Yalin, M.S. (1977): Mechanics of sediment transport (2nd ed.). Pergamon. 300pp.